

Phase Transitions of Heavy-Fermion Superconductors and Their Deviations from the Traditional BCS Superconductors

Shu-Wei Chang*

Department of Electrical and Computer Engineering,

University of Illinois at Urbana-Champaign, Urbana, IL, 61801, USA

(Dated: December 12, 2005)

Abstract

The heavy-fermion system has been discovered for more than twenty years. Despite a lot of efforts in the experimental investigations of these compounds, the origins of many related peculiar phenomena such as their unconventional superconductivity and magnetism still remain unknown. These compounds usually contain rare earth elements cerium and uranium whose outer f -shell electrons form a highly correlated system. They are usually characterized by the heavy mass of quasi-particles, large specific heat, and significant low-temperature magnetic susceptibility as well. In this essay, we will introduce the basic ideas and describe some experimental facts. Especially, we will focus on the differences between the heavy-fermion and traditional BCS superconductors.

*Electronic address: schang6@uiuc.edu

I. INTRODUCTION

The superconductivity of the first heavy-fermion material CeCu_2Si_2 was first discovered in 1979 [1]. This material has a significant specific heat γ of about 1100 mJ/mol K², and a large effective mass of the quasi-particles (formed by the 4f electrons) $m^* \sim 100 m_e$. After the discovery of this heavy-fermion material, many other compounds with a huge effective mass and specific heat were discovered, e.g., UBe_{13} (1983)[2] and UPt_3 (1984)[3]. Heavy-fermion compounds usually contain the rare earth elements cerium (Ce) and uranium (U). The element Ce has 4f electrons while the element U has 5f electrons. When forming compounds with other elements, these electrons lead to a narrow resonance with a high density of states within a narrow energy range due to the strong correlation between the conduction electronic states and the localized f moments. The origin of the large effective mass can be naively understood from this high density of states. Take degenerate electron gases in a typical metal for example. The usual dispersion relation (Energy versus wave vector) of a simple metal can be approximated by a parabola

$$E_k = \frac{\hbar^2 k^2}{2m^*}, \quad (1)$$

where k is the magnitude of the wave vector. Due to Pauli exclusion principle and assuming a weak-interacting or noninteracting case, the electrons (or fermionic quasi-particle) will occupy different states, and the corresponding distribution is characterized by the Fermi energy E_F and temperature T . For a give temperature T , if the fermi energy is much larger than the energy scale $k_B T$ (degenerate electron gas), where k_B is the Boltzman constant, only the electrons within the range of $k_B T$ below the Fermi energy E_F can be excited. Thus, as the temperature T increases, the internal energy ΔU gained compared with the zero-temperature electron gas and thus the specific heat capacity C_v can be written as

$$\begin{aligned} \Delta U &= \frac{N(k_B T)^2}{E_F} \propto D(E_F) T^2, \\ C_v &= \frac{\partial \Delta U}{\partial T} = 2k_B \frac{N k_B T}{E_F} \propto D(E_F) T, \end{aligned} \quad (2)$$

where N is the number of electrons in the gas and is a function of the Fermi energy E_F ; and $D(E_F)$ ($\propto N/E_F$) is the density of states at the Fermi energy. The proportionality to the density of states $D(E_F)$ at the Fermi energy in Eq. (2) is a general statement of a degenerate electron gas, not restricted to the parabolic dispersion relation in Eq. (1). However, the parabolic dispersion relation can gives us a heuristic guidance. The density of states $D(E_F)$ for a parabolic band is a function of the Fermi energy E_F and effective mass m^*

$$D(E_F) = \frac{1}{2\pi^2} \left(\frac{2m^*}{\hbar^2} \right)^{3/2} E_F^{1/2}. \quad (3)$$

From Eq. (3), we know a large effective mass leads to a significant density of states at the Fermi energy, and thus a huge heat capacity. We may turn the other way around– ”a significant density of states implies a huge effective mass,” even though this is not a precise statement.

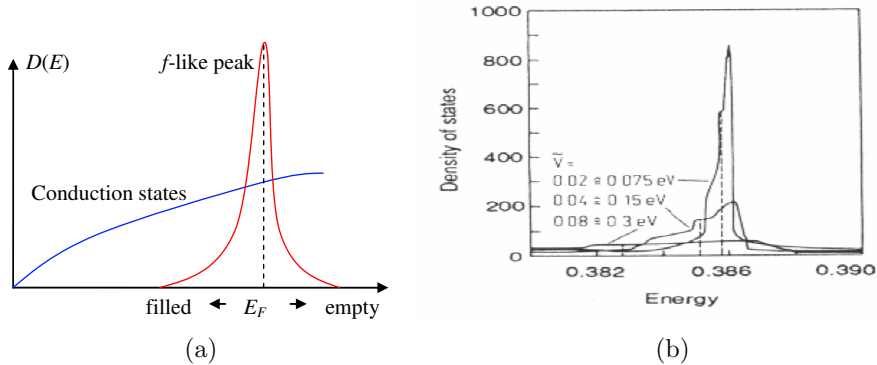


FIG. 1: The density of states due to the hybridization of the f electrons and conduction electronic states. (a) The peak in the density of states is f -like. The background density of states is due to the conduction band electronics states. (b) A calculation taking the strength of hybridization into consideration. After Ref. [4]

II. MORE ABOUT THE DENSITY OF STATES AND THE RELATION TO MAGNETISM

For the heavy fermion compounds, the huge density of states at the Fermi energy at a low temperature is due to the strong hybridization of the f electronic configuration of the elements Ce and U with the conduction electronic states from other elements. This single-particle hybridization results in a narrow f -like peak in the overall density states, see Fig. 1(a). A heuristic calculation taking the hybridization of the wave functions of the f electrons and conduction electrons into consideration is shown in Fig. 1(b) [4]. The coupling between the f -electronic state and conduction state results in a sharp resonance peak. At a low temperature, if the Fermi energy is located roughly around the center of the resonance peak, the high density of states at the Fermi energy leads to a very large effective mass and electronic heat capacity, as shown by Eq. (2). Usually, a narrower resonance peak causes a much higher density of states. The width of the resonance thus plays an important role in the physical parameters such as the effective mass and heat capacity.

If the width of the single particle resonance is smaller than the effective exchange energy of the spin-up and spin-down states, this single-particle resonance peak will be split into two. One of them corresponds to the spin-up electrons while the other corresponds to the spin-down electrons (see Fig. 2(a)). The occupation numbers of spin-up and spin-down electrons are thus not even. The spin-polarized f electrons are usually *quasi-bound* to the atoms donating them. This means those atoms may carry net magnetic moment via the coupling with these spin-polarized electrons. For Ce and U, the two split configurations ($4f^0$ and $4f^1$ for Ce and $5f^2$ and $5f^3$ for U) are not far apart. Both resonances contribute to the specific heat and thus heavy mass around the fermi energy.

The above is a single-particle view. When the many-body effect involving the magnetic interaction comes into play, the situation is further complicated. There are two cases related to it. The first one is a dilute limit at the low temperature caused by Kondo effect. In this situation, the local magnetic moments of the atoms are compensated by the anti-parallel spin polarization of conduction electrons due to anti-ferromagnetic coupling. The ground state is a nonmagnetic one [5]. This state has a binding energy $k_B T_k$, and a resonance caused

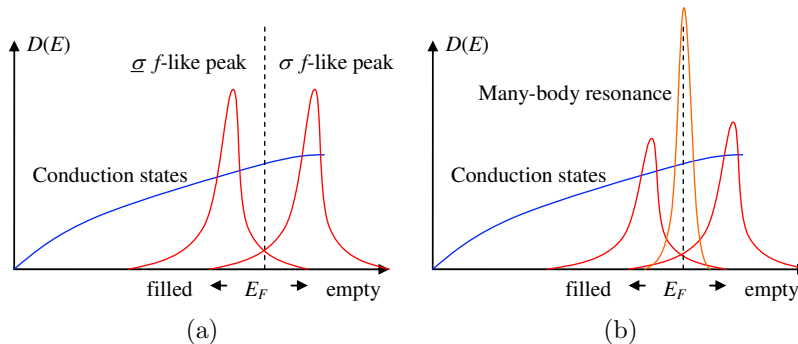


FIG. 2: (a) The density of states split into two resonance peaks due to the effective exchange interaction. One corresponds to σ (\uparrow or \downarrow), and the other corresponds to $\bar{\sigma}$ (the opposite of σ). (b) The Kondo effect makes the spin of the electron compensate the magnetic moment of the atoms. This state has a sharp resonance with a width of about $k_B T_k$ at the Fermi energy.

by this many-body interaction, as shown in Fig. 2(b). The resonance has a width of about $k_B T_k$ and is located at the Fermi energy. This resonance is caused by the many-body effect, and as temperature raises, its magnitude reduces and finally disappears due to the decrease in the compensation. This implies that in addition to the typical T dependence in the heat capacity C_v [see Eq. (3)], the “effective density of states” at the Fermi energy varies as the temperature changes. This is one of the characteristics about the heavy Fermion system: the dependence of the heat capacity below the superconducting temperature is far more complicated than a simple T -proportional dependence, though not necessarily due to the Kondo mechanism mentioned here or the traditional Bardeen-Cooper-Schrieffer (BCS) theory [6]. We will show some data on the heat capacity later. For a detail data collection on the early measurements of the heat capacity of the heavy fermion system and various strange temperature dependences, see Ref. [7].

The second case arises when the number of atoms with local magnetic moments (Ce or U) increases beyond the dilute limit. Electrons can no longer be thought of as quasi-bound to a particular atom though they still bear a significant f characteristic when they are close to these atoms. The electron will interact with many atoms via a Heisenberg-like spin-dependent interaction $J S_e \cdot S_{atom}$, where S_e is the spin of the electron while S_{atom} is the spin of the atom. The nature of the f electron hybridization makes the coupling constant J an anti-ferromagnetic sign. The interaction between the electrons and these atoms with magnetic moments bring about the effective coupling among the atoms themselves. These effective coupling is called the Ruderman-Kittel-Kasuya-Yosida (RKKY) coupling [8]. For a high concentration of the atoms with a magnetic moment but with a *random* distribution in the material, the RKKY interaction freezes these atoms into a *spin glass*.

The above two cases actually compete with each other. If the atoms with the magnetic moments are arranged in a periodic structure (Kondo lattice), the two cases will lead to either an ordered nonmagnetic phase (spin compensation) or a magnetic one (RKKY). Both phenomena seem to exist in the heavy fermion system. Another possible mechanism for the magnetically-ordered phase is caused by the spin density wave (SDW) of the conduction electron with a long-range order. Further, this spin-density wave is incommensurate, which means that the period of the spatial variation of the magnetic moment is not the same as that of the lattice, but rather determined by the Fermi surface.

III. SUPERCONDUCTIVITY IN THE HEAVY FERMION SYSTEM

Some of the heavy-fermion compounds become superconductive at a low temperature. The presence of superconductivity in this system then has brought about the reinspection to the BCS theory because in the traditional superconductors—the existence of the magnetic moment is not in favor of the superconductivity. It is believed that the pairing concept is still correct, but the pairing mechanism and symmetry may be different from those of the conventional BCS theory—the s-wave symmetry due to the effective attraction from virtual phonon exchange. For example, the superconductivity of the compound UPt₃ is suggested to be caused by the spin fluctuation, and the pairing symmetry is the p-wave symmetry, i.e. a triplet pairing ($l = 1, s = 1$). This suggestion was first made by fitting its heat capacity *above* T_c to the formula derived from the case of spin fluctuation [3]. Another example which implies the non s-wave pairing is the cubic power-law behavior the superconducting heat capacity $C_s(T)$ for UBe₁₃ [9]. The dependence on the cubic of temperature near zero temperature implied the p-wave pairing. However, for the similar material CeCu₂Si₂ and the same measurement, it was also reported the corresponding superconducting heat capacity $C_s(T)$ implied a *gapless* superconductivity [10] though it seemed that p-wave pairing can also fit the data pretty well. Due to the lack of a high-quality single crystal CeCu₂Si₂, many properties about this material so far are still not accurate enough for a conclusive judgement.

Also, there are examples showing that a significant magnetism and superconductivity can be coexistent, contrary to the concept that the superconductivity can only coexist with a small magnetic moment in the heavy fermion system. The compounds UPd₂Al₃ [11] and UNi₂Al₃ [12] are such examples which show a significant magnetic moment below the superconductivity transition temperature, implying an interplay between the magnetic order parameter and superconductivity order parameter. The ordered magnetic moment μ_s of the compound UPd₂Al₃ is about $0.85 \mu_B$. This value is about two order of magnitude larger than the small magnetic moment ($\sim 0.01 \mu_B$) which was considered as the limit for the simultaneous presences of the magnetic and superconductivity ground states.

So far, the mechanisms leading to the superconductivity in the heavy-fermion system are not clear for each compound. Thus, we cannot develop a theory which can explain every detail of the experiments from the very beginning. However, we should be able to predict what phenomenon we can see if the interaction with a certain symmetry is responsible for the superconductivity. Since we don't have a correct Hamiltonian to begin with, we have to include a certain degree of phenomenology into the theory. Landau's free energy is a good starting point near the temperature of the superconductivity transition. Many thermodynamic quantities such as the specific heat near the transition temperature T_c can be calculated from this theory as long as the functional form of the Landau's free energy obeys the correct symmetry of the compound, i.e., the symmetry of the lattice *point group*. Also, by minimizing the Landau's free energy, we would be able to get a rough picture on what the phase diagram looks like even though the critical exponents near those critical points may not be correct. It has been shown that for traditional superconductors, the microscopic BCS theory can be simplified to Landau's theory near the transition temperature [13]. With the same idea, Landau's theories which include the appropriate symmetries for different materials should be able to reveal some information of the heavy-fermion system. A detail description using this phenomenal approach but including the lattice symmetry (the symmetry of the crystal field) can be found in Ref. [14]. Basically, the group-theoretical ap-

proach is needed in writing down Landau's free energy near the superconductivity transition temperature.

Here, we briefly introduce the calculation of the order parameter (gap function) near T_c for a general point group symmetry. The goal is to at least get an idea what s-wave, p-wave...and so on actually mean. For more details, please refer to Ref. [14]. As mentioned above, we have no idea what the effective interaction between the electrons is and can only assume a phenomenological attractive interaction V whose origin requires further inspections. All what we know is the symmetry of the potential V . Assume that spin is a good quantum number for the *single-particle* part of the Hamiltonian first. The starting Hamiltonian H can be written as

$$H = \sum_{\mathbf{k},s} \varepsilon(\mathbf{k}) a_{\mathbf{k}s}^\dagger a_{\mathbf{k}s} + \frac{1}{2} \sum_{\mathbf{k},\mathbf{k}',s_1,s_2,s_3,s_4} V_{s_1,s_2,s_3,s_4}(\mathbf{k},\mathbf{k}') a_{-\mathbf{k}s_1}^\dagger a_{\mathbf{k}s_2}^\dagger a_{\mathbf{k}'s_3} a_{-\mathbf{k}'s_4},$$

$$V_{s_1,s_2,s_3,s_4}(\mathbf{k},\mathbf{k}') \equiv \langle -\mathbf{k},s_1; \mathbf{k},s_2 | V | -\mathbf{k}',s_4; \mathbf{k}',s_3 \rangle, \quad (4)$$

where $\varepsilon(\mathbf{k})$ is the energy relative to the chemical potential for a particular band; and a_{\dots} and a_{\dots}^\dagger are the annihilation and creation operators with a corresponding labels.

Due to Pauli's exclusion principle, the matrix element $V_{s_1,s_2,s_3,s_4}(\mathbf{k},\mathbf{k}')$ satisfies the following symmetry: $V_{s_1,s_2,s_3,s_4}(\mathbf{k},\mathbf{k}') = -V_{s_2,s_1,s_3,s_4}(-\mathbf{k},\mathbf{k}') = -V_{s_1,s_2,s_4,s_3}(\mathbf{k},-\mathbf{k}') = V_{s_4,s_3,s_2,s_1}(\mathbf{k}',\mathbf{k})$. In the mean-field sense, the matrix elements of the order parameter are

$$\hat{\Delta}(\pm\mathbf{k}) = \begin{pmatrix} \Delta_{\uparrow\uparrow}(\pm\mathbf{k}) & \Delta_{\uparrow\downarrow}(\pm\mathbf{k}) \\ \Delta_{\downarrow\uparrow}(\pm\mathbf{k}) & \Delta_{\downarrow\downarrow}(\pm\mathbf{k}) \end{pmatrix},$$

$$\Delta_{ss'}(\mathbf{k}) = - \sum_{\mathbf{k}',s_3,s_4} V_{s'ss_3s_4}(\mathbf{k}') \langle a_{\mathbf{k}',s_3} a_{-\mathbf{k}'s_4} \rangle,$$

$$\Delta_{ss'}(-\mathbf{k}) = - \sum_{\mathbf{k}',s_1,s_2} V_{s_1s_2s's}(\mathbf{k}',\mathbf{k}) \langle a_{-\mathbf{k}',s_1}^\dagger a_{-\mathbf{k}'s_2}^\dagger \rangle. \quad (5)$$

The effective mean-field Hamiltonian \bar{H} is then written as

$$\bar{H} = \sum_{\mathbf{k},s} \varepsilon(\mathbf{k}) a_{\mathbf{k}s}^\dagger a_{\mathbf{k}s} + \frac{1}{2} \sum_{\mathbf{k},s_1,s_2} [\Delta_{s_1s_2}(\mathbf{k}) a_{\mathbf{k}s_1}^\dagger a_{-\mathbf{k}s_2}^\dagger - \Delta_{s_1s_2}^*(-\mathbf{k}) a_{-\mathbf{k}s_1} a_{\mathbf{k}s_2}]. \quad (6)$$

When paring the spins of the two electrons, the singlet and triplet spin states are both possible depending on their symmetries in the \mathbf{k} space. The singlet or triplet pairing will result in different forms of order parameter matrices

$$\hat{\Delta}(\mathbf{k}) = i\sigma_y \psi(\mathbf{k}) = \begin{pmatrix} 0 & \psi(\mathbf{k}) \\ -\psi(\mathbf{k}) & 0 \end{pmatrix} \text{ for singlet,}$$

$$\hat{\Delta}(\mathbf{k}) = i[\mathbf{d}(\mathbf{k}) \cdot \boldsymbol{\sigma}] \sigma_y = \begin{pmatrix} -d_x(\mathbf{k}) + id_y(\mathbf{k}) & d_z(\mathbf{k}) \\ d_z(\mathbf{k}) & d_x(\mathbf{k}) + id_y(\mathbf{k}) \end{pmatrix} \text{ for triplet,} \quad (7)$$

where $\psi(\mathbf{k})$ is an *even* function of the wave vector \mathbf{k} ; $\mathbf{d}(\mathbf{k}) [= d_x(\mathbf{k})\hat{x} + d_y(\mathbf{k})\hat{y} + d_z(\mathbf{k})\hat{z}]$ transforms like a *complex vector function*. After the Bogoliubov transformation to the quasi-particle picture, the order-parameter matrix satisfies the matrix form of the self-consistent

gap equation assuming that the occupation number is a Fermi-Dirac distribution

$$\Delta_{ss'}(\mathbf{k}) = - \sum_{\mathbf{k}', s_3, s_4} V_{s's_3s_4}(\mathbf{k}, \mathbf{k}') F_{s_3, s_4}(\mathbf{k}', \beta = 1/k_B T), \quad (8)$$

where the matrix element $F_{s_3, s_4}(\mathbf{k}', \beta)$ in the singlet case is

$$\hat{F}(\mathbf{k}, \beta) = \frac{\hat{\Delta}(\mathbf{k})}{2E_{\mathbf{k}}} \tanh(\beta E_{\mathbf{k}}), \quad E_{\mathbf{k}} = \sqrt{\varepsilon^2(\mathbf{k}) + \frac{1}{2} \text{tr} \Delta(\mathbf{k}) \Delta(\mathbf{k})^\dagger}, \quad (9)$$

and for triplet case is

$$\hat{F}(\mathbf{k}, \beta) = \left\{ \frac{1}{2E_{\mathbf{k}+}} \left[\mathbf{d} + \frac{\mathbf{q} \times \mathbf{d}}{|\mathbf{q}|} \right] \tanh\left(\frac{1}{2} \beta E_{\mathbf{k}+}\right) + \frac{1}{2E_{\mathbf{k}-}} \left[\mathbf{d} - \frac{\mathbf{q} \times \mathbf{d}}{|\mathbf{q}|} \right] \tanh\left(\frac{1}{2} \beta E_{\mathbf{k}-}\right) \right\},$$

$$\mathbf{q} = i(\mathbf{d} \times \mathbf{d}^*), \quad E_{\mathbf{k}\pm} = \sqrt{\varepsilon^2(\mathbf{k}) + |\mathbf{d}(\mathbf{k})|^2 \pm |\mathbf{q}(\mathbf{k})|}. \quad (10)$$

Just below the first critical temperature T_c , at which the first phase other than the high temperature phase occurs, the order parameter is small. Thus, we can linearize Eq. (10) with respect to the order parameter and obtain the following equation:

$$v \Delta_{s_1 s_2}(\mathbf{k}) = - \sum_{s_3, s_4} \langle V_{s_2 s_1 s_3 s_4}(\mathbf{k}, \mathbf{k}') \Delta_{s_3 s_4}(\mathbf{k}') \rangle_{\mathbf{k}'},$$

$$\frac{1}{v} = D(E_F) \int_0^{\varepsilon_c} d\varepsilon \frac{\tanh(\beta_c \varepsilon_k)}{\varepsilon(\mathbf{k})} \sim \ln(1.14 \beta_c \varepsilon_c), \quad (11)$$

where ε_c is the upper bound of the interaction, and $\langle \dots \rangle_{\mathbf{k}}$ means the average over the \mathbf{k} space. Eq. (11) is an eigenvalue problem with eigenvalue v . Thus, once the eigenvalue is determined, we can then work back to find the critical temperature T_c . From Eq. (11), if the rotational symmetry is present in the Hamiltonian without the *spin-orbital coupling*, the function $\psi(\mathbf{k})$ and the vector function $\mathbf{d}(\mathbf{k})$ are characterized by the even and odd angular momentum quantum numbers, respectively. They are expanded as

$$\psi(\mathbf{k}) = \sum_m c_m Y_{lm}(\hat{\mathbf{k}}) \quad (l \text{ even}), \quad \mathbf{d}(\mathbf{k}) = \sum_{m, \hat{\mathbf{n}}=\hat{x}, \hat{y}, \hat{z}} Y_{lm}(\hat{\mathbf{k}}) \hat{\mathbf{n}} \quad (l \text{ odd}), \quad (12)$$

where $Y_{lm}(\hat{\mathbf{k}})$ is the spherical harmonic functions. Now, we can already see some hints of the origin of the terminology for the electron pairing, though it is not the whole story yet. The even angular momentum quantum numbers correspond to “s-wave” ($l = 0$), “d-wave” ($l = 2$)...etc for the spin singlet while the odd angular momentum quantum numbers correspond to “p-wave” ($l = 1$) and so on for the spin triplet.

Let us turn on the spin-orbital coupling and crystal field one by one. If the spin-orbital coupling ($\propto \mathbf{L} \cdot \mathbf{S}$) is turned on, the group operations on the wave vector \mathbf{k} and on the spin space are no longer independent of each other. In this case, instead of the single angular momentum quantum number l , we should consider the total angular momentum quantum number j and the corresponding operator $\mathbf{J} = \mathbf{L} + \mathbf{S}$. For the spin singlet, we have to consider the subspace $j = l$, and for the spin triplet, we have to consider the subspaces $j = l - 1, l, l + 1$. The calculation of the order parameter matrix cannot be reduced to the expansion of a single scalar shown in Eq. (12). The Clebsh-Gordon procedure

is usually carried out to find the basis functions, which are usually the mixture of the spin and the orbital part. Note that although j maybe a good quantum number, however, the bases obtained from the Clebsh-Gordon procedure may not be the eigenfunctions of the total Hamiltonian. For different pairs of quantum numbers (l, s) and (l', s') , the addition of the angular momenta from these two pairs may both lead to the same total momentum angular momentum quantum number j . The interaction V will mix the two sets of bases obtained from the subspaces characterized by (l, s) and (l', s') . Thus, the order-parameter matrix, though can be characterized by the quantum number j , still contains a complicated expansion of the wave vector.

If the crystal field is turned on, the symmetry of the lattice point group then comes into play. In this case, since there are only a finite number of irreducible representations of the lattice point group, the possible basis functions for $\psi(\mathbf{k})$ and $\mathbf{d}(\mathbf{k})$ are limited. Suppose for a given representation Γ , we have m basis functions $\hat{\Delta}(\Gamma, m; \mathbf{k})$. The order-parameter matrix then can be written as

$$\hat{\Delta}(\mathbf{k}) = \sum_m \eta(\Gamma, m) \hat{\Delta}(\Gamma, m; \mathbf{k}), \quad (13)$$

where $\eta(\Gamma, m)$ is the expansion coefficient. The detail of the basis function for some representations can be found in Ref. [14]. Up to this stage, we should give a *not-so-precise* definition of the l -wave pairing. If a basis function contains terms as follows:

$$\hat{\Delta}(\Gamma, m; \mathbf{k}) = \dots + k_x^\alpha k_y^\beta k_z^\gamma + \dots, \quad l = \alpha + \beta + \gamma, \quad (14)$$

we then call it l -wave pairing. There are exceptions, such as the totally-symmetric but nonconstant function, which is called *extended s-wave pairing*.

It is important to know what the impact of the pairing symmetry on the heat capacity of the heavy-fermion superconductors is. We assume that the concept of the cooper pair is still valid in these heavy-fermion superconductors. Thus, we can classify the order parameter—the gap function by the crystal symmetry. One of the virtue of the microscopic theory of the BCS theory is the prediction of a heat capacity with a temperature dependence $T^{-2} \exp(-\Delta(T)/k_B T)$ far below T_c . The formation of an *isotropic* (s-wave) gap on the Fermi surface is a key element to the proportionality of the temperature-dependent exponential. On the other hand, if there are nodes or zero lines of the gap function present on the Fermi surface or even no formation of the gap at all (gapless superconductors), the behavior of the heat capacity will be completely different from that predicted by the BCS theory. The power-law dependence of the heat capacity replaces the exponential one. Experimentally, measuring the superconducting heat capacity below T_c is one of the ways to test the symmetry of the gap function even though it usually does not lead to a firm conclusion. Here, we briefly mention the temperature dependence of the heat capacity when nodes or zero lines are present in the gap function.

The temperature-dependent exponential term in the s-wave superconductivity heat capacity can be naively understood as the Boltzman factor which enters the calculation of the “partition function” of the quasi-particle states. Since the gap is everywhere on the Fermi surface, there is no easy way for the quasi particle to be excited. However, if nodes or zero lines appear on the Fermi surface, quasi-particles may be easily excited near these zeros on the Fermi surface. The superconductivity heat capacity $C_s(T)$ is

$$C_s(T) = \frac{1}{T} \int_0^\infty dE D_{q.p.}(E) E^2 \left[-\frac{df(E)}{dE} \right] \quad (T \ll T_c), \quad (15)$$

where $f(E)$ is the Fermi-Dirac distribution, and $D_{q.p.}(E)$ is the quasi-particle density of states. Under different topologies of the Fermi surface, the dependence on the temperature T can be written as

$$C_s(T) \propto \begin{cases} T & \text{gapless} \\ T^2 & \text{linezeros} \\ T^3 & \text{pointzero} \end{cases} . \quad (16)$$

For example, in the p-wave pairing symmetry, zero node appears on the Fermi surface. Thus, the cubic behavior of the heat capacitance is considered as the sign of p-wave pairing, as mentioned previously for the compound UBe_{13} .

IV. EXPERIMENTAL FACTS

In this section, we show some experimental results and briefly discuss the theoretical possibilities indicated by them. The heat capacity, magnetic susceptibility, and resistivity measurements will be our concerns. We will focus on the heavy-fermion compounds which become superconductive at a low temperature though many other heavy-fermion compounds also exhibit many unusual properties in these measurements.

A. Heat Capacity

The heat capacity in absence of phase transition in a metal far below the Debye temperature but above the T_c is usually written as

$$\frac{C_v(T)}{T} = \gamma + \beta T^2, \quad (17)$$

where the parameters γ and β describe the contributions from electrons and the lattice vibration, respectively. Below the transition temperature, the parts in addition to these contributions are attributed to certain kind of phase transitions, usually the emergence of superconducting phase. In this case, the parameter γ is treated as temperature-dependent below T_c , and many people plot $C_v(T)/T$ versus T^2 to study how significant the deviation from the straight line described by Eq. (17) is, though this is not always done. Figure 3(a), (b), (c) shows C_v/T or C_v for CuSi_2Cl_2 [15], UBe_{13} [16], and UPt_3 [17]. As mentioned above, the measurements of CuSi_2Cl_2 are very sample-dependent. Thus, from the heat capacity, we can only say that there is a certain kind of transition, possibly the emergence of superconductivity, and its pairing symmetry is not the conventional one, maybe p-wave or gapless. Comparing with CuSi_2Cl_2 , the result of UBe_{13} is much more conclusive due to a less sample uncertainty. A striking fact about UBe_{13} takes place in its phase diagram when some of the atom U is replaced by the element thorium (Th). As the concentration of doping increases, the critical temperature first drops, but later, increases again. In addition to it, another phase with a lower T_c emerges between $x = 0.018 - 0.045$ [19, 20], as shown in Fig. 3(d) [18]. The transition at the lower critical temperature is suggested to be a second superconducting state due to the coupling to the spin-density wave [18, 21, 22]. The presence of the SDW generates a second superconducting order parameter, and this second superconducting state may have an even larger condensation energy. For UPt_3 , there are two phases corresponding to different transition temperatures [23]. These two phases may

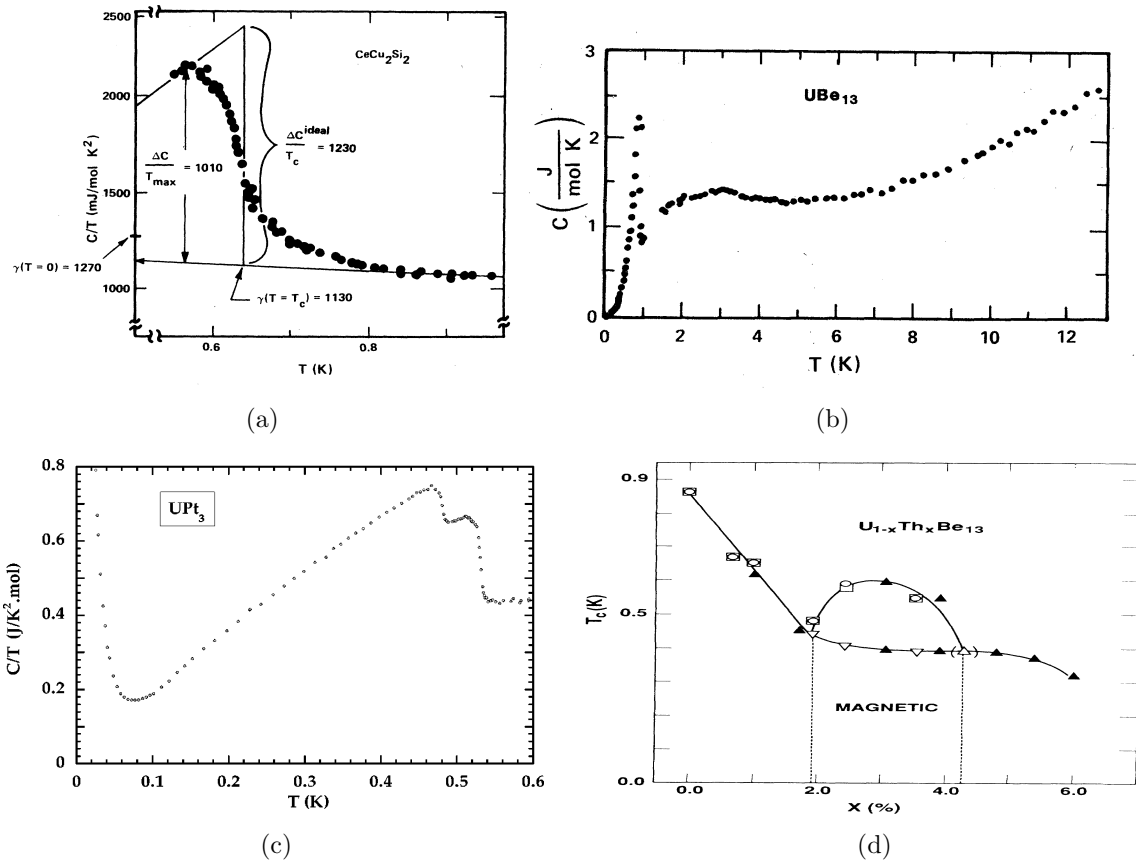


FIG. 3: Heat capacities of various heavy-fermion compounds as a function of temperature. (a) CeCu_2Si_2 [15]. (b) UBe_{13} [16]. (c) UPt_3 [17]. (d) The phase diagram of $\text{U}_{1-x}\text{Th}_x\text{Be}_{13}$ [18]

be caused by the lifting of a certain degeneracy, as suggested that at a high pressure, the two transition temperatures merge into one [24]. The early measurement of the heat capacity could not resolve these two phases [3], but the availability of a high-quality single crystal of UPt_3 made it possible to distinguish the two phases. Also, above the transition temperature, C_v/T can be fitted by the following equation

$$C_v(T) = \gamma T + \beta T^3 + \delta T^3 \ln T. \quad (18)$$

This form of heat capacity is a strong indication of the spin fluctuation, implying that the superconductivity of UPt_3 is mediated by the spin fluctuation [3]. Also, UPt_3 is one of the few examples in the heavy-fermion system whose material properties do not deviate significantly from one measurement to another. For a detailed review on UPt_3 , see Ref. [25].

B. Magnetic Susceptibility

The inverses of the magnetic susceptibilities $\chi^{-1}(T)$ of the materials CeCu_2Si_2 [26], UBe_{13} [16], and UPt_3 [27] are shown in Fig. (4). At a high temperature, all of the three susceptibilities can be described by the Curie-Weiss law $\chi(T) \propto (T + \Theta)^{-1}$, $\Theta < 0$, and they exhibit quite large magnetic susceptibilities at low temperatures (small $\chi^{-1}(T)$ at a low tem-

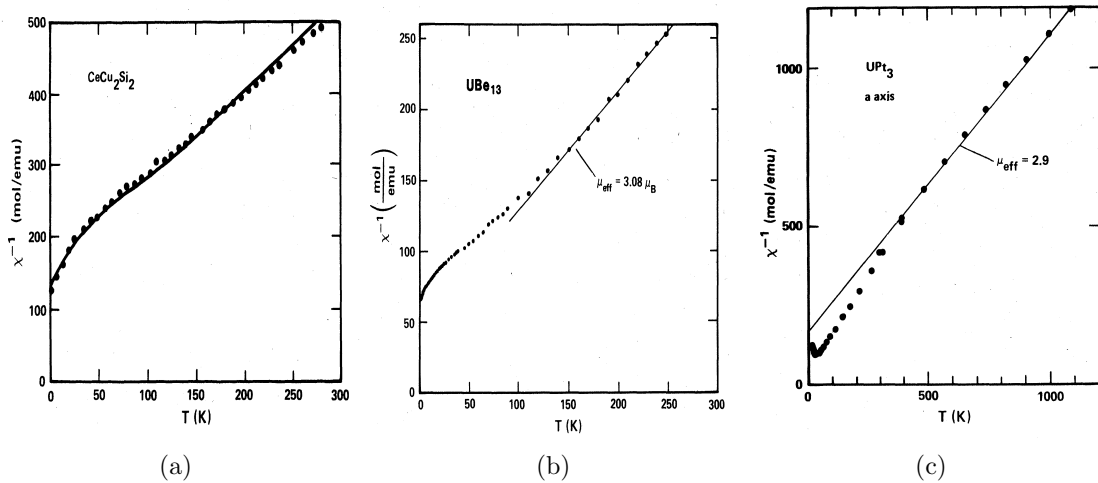
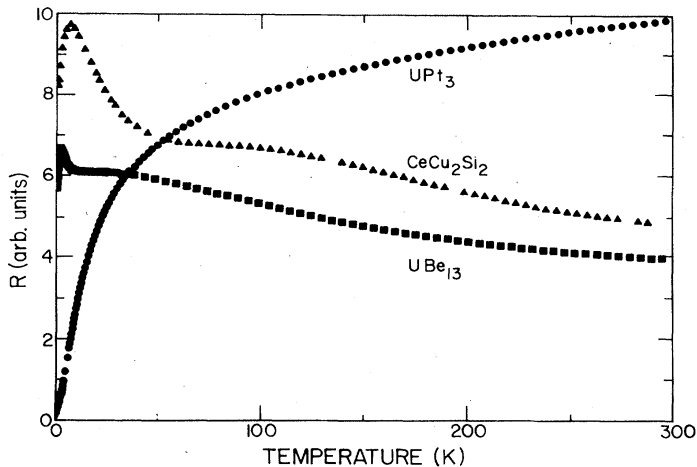


FIG. 4: The inverses of the magnetic susceptibilities $\chi(T)^{-1}$ of various heavy fermion system as a function of temperature. (a) CuSi_2Cl_2 [26]. (b) UBe_{13} [16]. (c) UPt_3 [27].

perature). The effective magnetic moments μ_{eff} corresponding to these susceptibilities are quite large ($\sim 2.61 \mu_B$ for CuSi_2Cl_2 , $\sim 3.08 \mu_B$ for UBe_{13} , and $\sim 2.9 \mu_B$ for UPt_3). Again, due to a larger variation of the sample quality, the compound CuSi_2Cl_2 has a significant variation in the magnetic susceptibility. To have a rough idea how significant the susceptibilities of these materials are at a low temperature, we compare them with that of the f -electron atom plutonium Pu which is closet to being magnetic. The magnetic susceptibility of Pu at the zero temperature is 0.5×10^{-3} emu/mol G. The magnetic susceptibility of CuSi_2Cl_2 at a low temperature, which is among the smallest ones in the heavy-fermion system, is about 8×10^{-3} emu/mol G. This value is significantly larger than that of Pu. The large magnetic susceptibility may be caused by the Kondo effect which results in the compensation of the local magnetic moments by the conduction electrons as mentioned earlier, or by another mechanism which describes the competition between two f -electron ground states [26]. One of the ground state is magnetic while the other is nonmagnetic. It is interesting to note that at a low temperature, the deviation of the high-temperature behavior of the susceptibility of the compound UPt_3 is different from those of CuSi_2Cl_2 and UBe_{13} . A minimum exists in the inverse of magnetic susceptibility $\chi^{-1}(T)$. This phenomenon suggests that the superconductivity and magnetic properties of UPt_3 are different from the other two. Actually, the compound UPt_3 exhibits many different properties from other heavy-fermion compounds at a low temperature, not necessarily restricted to the other two compounds mentioned here. This implies that the pairing mechanism compound UPt_3 may also be unique.

C. Resistivity

Figure 5 shows the resistivities of CuSi_2Cl_2 [28], UBe_{13} [2], and UPt_3 [3]. At a very low temperature, the resistivities all become much smaller than their high-temperature counterparts. Note that there are global maxima for both the resistivities of CuSi_2Cl_2 and UBe_{13} . These local maxima are caused by the Kondo-lattice scattering which increases as the temperature decreases. After those global maxima, the resistivities soon decrease. There are also side shoulders on the resistivities of CuSi_2Cl_2 and UBe_{13} at the higher-temperature sides



(a)

FIG. 5: The resistivities of CuSi_2Cl_2 [28], UBe_{13} [2], and UPt_3 [3] as a function of temperature.

of the global maxima. They are caused by the crystal-field effect. Note that this local maximum is absent in the resistivity of UPt_3 . The resistivity goes to zero monolithically as the temperature decreases. This again shows that the material UPt_3 is different from the other materials. The low temperature behavior of the resistivity can be usually described by a T^2 behavior. This T^2 behavior may be caused by the Fermi-liquid theory. However, many other mechanisms can also cause this temperature dependence. Other measurements on different material properties have to be used to make a better judgement.

D. Other Measurements

Some other approaches can be used to test the differences of the heavy fermion materials below and above various transition temperatures. For example, both nuclear magnetic resonance (NMR) relaxation rate and muon spin rotation and relaxation (μSR) techniques have found their positions in the field of the heavy-fermion system. Both of them sense the change of the local magnetic field in the material corresponding to different phases. NMR technique utilizes the nuclear magnetic moment while the μSR technique uses the spin polarizations of positive muon μ^+ . For a detailed review on the investigation of the μSR technique on the heavy fermion system, see Ref. [29].

NMR relaxation rate can also be used to test the pairing symmetry at different temperatures. This technique is first developed to test the standard BCS superconductors [30] and can be extended to others with unconventional pairing mechanisms. The NMR relaxation time $T_{1,s}^{\text{NMR}}(T)$ in the superconducting phase contains the information of the order parameter on the Fermi surface. The corresponding temperature dependence is listed below:

$$\frac{T_{1,n}^{\text{NMR}}(T)}{T_{1,s}^{\text{NMR}}(T)} \propto \begin{cases} T & \text{gapless} \\ T^3 & \text{linezeros} \\ T^5 & \text{pointzero} \end{cases}, \quad (19)$$

where $T_{1,n}^{NMR}(T)$ is the NMR relaxation time in the normal state.

Impurity substitution is also a tool to inspect the heavy-fermion materials. However, the physical properties of the heavy-fermion materials are usually very sensitive to these small variations of the substitution parameters, which also make the accurate measurements very hard (recall the case of CeCu_2Si_2). Thus, they are usually used as an auxiliary tool only.

V. CONCLUSION

The heavy-fermion system is a complicated system but also contains rich physics. The superconductivity in the heavy-fermion is probably not the s-wave pairing described by the traditional BCS theory. The power-law behaviors in many measurements are strong evidence of the non-trivial pairing symmetry though more efforts have to be devoted to settle down the discrepancies between many measurements. Parts of the confusion come from the uncertainty of the samples. The others come from the lack of a comprehensive theory which can be applied to different materials. The interplay of the intrinsic magnetism and the superconductivity is another part which makes the heavy-fermion superconductivity fascinating. This phenomenon is absent in the traditional BCS superconductors. There is still a long way to go for the heavy-fermion system since many questions still remain open, especially on the microscopic mechanism of the superconductivity and its relation to the magnetism of the material.

-
- [1] F. Steglich, J. Aarts, C. D. Bredl, W. Lieke, D. Meschede, W. Franz, and H. Schafer, Phys. Rev. Lett. **43**, 1892 (1979).
 - [2] H. R. Ott, H. Rudigier, Z. Fisk, and J. L. Smith, Phys. Rev. Lett. **50**, 1595 (1983).
 - [3] G. R. Stewart, Z. Fisk, J. O. Willis, and J. L. Smith, Phys. Rev. Lett. **52**, 679 (1984).
 - [4] U. Hoffmann and J. Keller, Z. Phys. B. Cond. Matter **74**, 499 (1989).
 - [5] A. M. Tsvetick and P. B. Wiegmann, Adv. Phys. **32**, 453 (1983).
 - [6] J. Bardeen, L. N. Cooper, and J. R. Schrieffer, Phys. Rev. **108**, 1175 (1957).
 - [7] G. R. Stewart, Rev. Mod. Phys. **56**, 755 (1984).
 - [8] M. A. Ruderman and C. Kittel, Phys. Rev. **96**, 99 (1954).
 - [9] H. R. Ott, H. Rudigier, T. M. Rice, K. Ueda, Z. Fisk, and J. L. Smith, Phys. Rev. Lett. **52**, 1915 (1984).
 - [10] C. D. Bredl, H. Spille, U. Rauchschwalbe, W. Lieke, F. Steglich, G. Cordier, W. Assmus, and M. H. and, J. Magn. Magn. Mater **31-34**, 373 (1983).
 - [11] C. Geibel, C. Schank, S. Thies, H. Kitazawa, C. D. Bredl, A. Bohm, M. Rau, A. Grauel, R. Caspary, R. Helfrich, et al., Z. Phys. B **84**, 1 (1991).
 - [12] C. Geibel, S. Thies, D. Kaczorowski, A. Mehner, A. Grauel, B. Seidel, U. Ahlheim, R. Helfrich, K. Petersen, C. D. Bredl, et al., Z. Phys. B **83**, 305 (1991).
 - [13] L. P. Gorkov, Sov. Phys. JETP **9**, 1364 (1959).
 - [14] M. Sigrist and K. Ueda, Rev. of Mod. Phys **63**, 239 (1991).
 - [15] W. Lieke, U. Rauchschwalbe, C. D. Bredl, F. S. anf J. Arts, and F. R. de Boer, J. Appl. Phys **53** (1982).
 - [16] H. R. Ott, H. Rudigier, Z. Fisk, and J. L. Smith, *Moment formation in Solids* (Plenum, New York, 1984).

- [17] J. P. brison, N. Keller, P. Lejay, J. L. Tholence, A. Huxley, N. R. Bernhoeft, A. Buzdin, B. Fak, J. Flouquet, L. Schmidt, et al., *J. Low. Temp. Phys.* **95**, 145 (1994).
- [18] R. H. Heffner, J. L. Smith, J. O. Willis, P. Birrer, C. Baines, F. N. Gygax, B. Hitti, E. Lippelt, H. R. Ott, A. Schenck, et al., *Phys. Rev. Lett.* **65**, 2816 (1990).
- [19] H. R. Ott, H. Rudigier, E. Felder, Z. Fisk, and J. L. Smith, *Phys. Rev. B* **33**, 126 (1986).
- [20] E. Felder, A. Bernasconi, H. R. Ott, Z. Fisk, and L. J. Smith, *Physica C* **162-164** (1989).
- [21] M. Gulacsi and Z. Gulacsi, *Phys. Rev. B* **39**, 12352 (1989).
- [22] M. Ozaki and K. Machida, *Phys. Rev. B* **39**, 4145 (1989).
- [23] R. A. Fisher, S. Kim, B. F. Woodfield, N. E. Phillips, L. Taillefer, K. Hasselbach, J. Flouquet, A. L. Giorgi, and J. L. Smith, *Phys. Rev. Lett.* **62**, 1411 (1989).
- [24] T. Trappmann, H. V. Lohneysen, and L. Taillefer, *Phys. Rev. B* **43**, 13714 (1991).
- [25] R. Joynt and L. Taillefer, *Rev. Mod. Phys.* **74**, 235 (2002).
- [26] B. C. Sales and R. Viswanathan, *J. Low Temp. Phys.* **23**, 499 (1976).
- [27] P. H. Frings, J. J. M. Franse, F. R. de Boer, and A. Menovsky, *J. Magn. Magn. Mater.* **31-34**, 240 (1983).
- [28] G. R. Stewart, Z. Fisk, and J. O. Willis, *Phys. Rev. B.* **28**, 172 (1983).
- [29] A. Amato, *Rev, Mod. Phys.* **69**, 1119 (1997).
- [30] L. C. Hebel and C. P. Slitcher, *Phys. Rev.* **116**, 79 (1959).